

SIMCO: SIMILARITY-BASED OBJECT COUNTING

Marco Godi, Christian Joppi, Andrea Giachetti, Marco Cristani

University of Verona, Department of Computer Science, Strada le Grazie, 15

ABSTRACT

We present SIMCO, the first agnostic multi-class object counting approach. SIMCO starts by detecting foreground objects through a novel Mask RCNN-based architecture trained beforehand (just once) on a brand-new synthetic 2D shape dataset, *InShape*; the idea is to highlight every object resembling a primitive 2D shape (circle, square, rectangle, etc.). Each object detected is described by a low-dimensional embedding, obtained from a novel similarity-based head branch; this latter implements a triplet loss, encouraging similar objects (same 2D shape + color and scale) to map close. Subsequently, SIMCO uses this embedding for clustering, so that different types of objects can emerge and be counted, making SIMCO the very first multi-class unsupervised counter. Experiments show that SIMCO provides state-of-the-art scores on counting benchmarks and that it can also help in many challenging image understanding tasks.

Index Terms— Object counting, 2D shape dataset

1. INTRODUCTION

Most approaches for counting similar objects in images assume a single object class [1, 2, 3, 4]; when is not, ad-hoc learning is necessary [5, 6]. None of them are truly agnostic and multi-class, i.e., able to capture generic repeated patterns of different type without any tuning. Counting approaches are based on regression ([7]) or density estimation ([3, 1]); here we focus on counting by detection [6, 8] so the counted objects are individually detected first.

Research on agnostic counting is important in many fields. It serves for visual question answering [9, 10], where counting questions could be made on too-specific entities, outside the semantic span of the available classes [11] (e.g. “What is the most occurrent thing?” in Fig. 1). In representation learning, unsupervised counting of visual primitives (i.e., visual “things”) is crucial to obtain a rich image representation [3, 12, 13]. Counting is a hot topic in cognitive robotics [14, 15], where autonomous agents learn by separating sensory input into a finite number of classes (without a precise semantics), building a classification system that counts on each of them.

Application-wise, agnostic counting may help the manual tagging of training images [16], providing a starting guess for the annotator on single- [17, 18] or multi-spectral [19, 20]

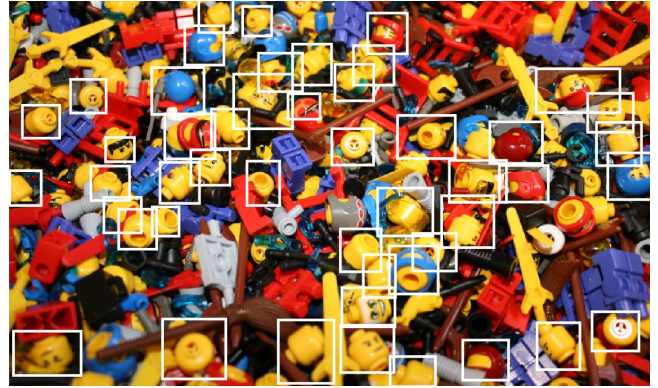


Fig. 1: SIMCO on visual question answering: the most occurrent object? SIMCO finds 47 LEGO heads.

images. Inpainting filters may benefit from a magic wand capturing repeated instances to remove. Examples of these applications are shown in Sec. 3.

In this paper, we present the SIMilarity-based object Counting (SIMCO) approach, which is completely agnostic, i.e. with no need of any *ad-hoc* class-specific fine tuning, and multi-class, i.e. finding different types of repeated patterns. Two main ideas characterise SIMCO.

First, every object to be counted is considered as a specialization of a basic 2D shape: this is particularly true with many and small objects [21, 22] (see Fig. 1: LEGO heads can be approximated as circles). SIMCO incorporates this idea building upon a novel Mask-RCNN-based classifier, fine-tuned just once on a novel synthetic shape dataset, *InShape*.

The second idea is that, leveraging on the 2D shape approximation of objects, one can naturally perform unsupervised grouping of the detected objects (grouping circles with circles etc.), discovering *different* types of repeated entities (without resorting to a particular set of classes). SIMCO realizes this with a head branch in the network architecture implementing triplet losses, which provides a 64-dim embedding that maps objects close if they share the same shape class plus some appearance attributes. Affinity propagation clustering [23] finds groups over this embedding.

Results are state-of-the-art on cell counting benchmarks [24], and on the RepTile dataset [6], explicitly suited for agnostic object counting. Qualitative results illustrate some of the many scenarios where SIMCO can definitely help.

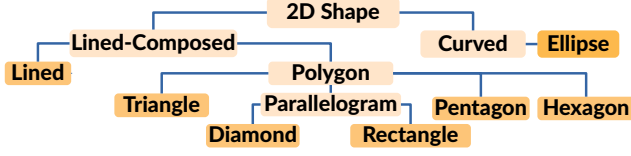


Fig. 2: 2D shape ontology inspired by [28].

2. THE SIMCO APPROACH

The SIMCO two-step algorithm uses a deep architecture which is trained just once, and that generalizes to whichever image. It is the first multi-class counting by detection approach in this sense: the first step (“Detection”, Sec. 2.1) provides a single class of generic foreground objects (that can be counted if no multi-class specification is needed); each detected object is described by a 64-dimensional neural feature vector. The second step (“Clustering”, Sec. 2.2) groups the detections into clusters so that each resulting cluster is a different visual “thing” with its own count.

2.1. SIMCO detection

SIMCO builds upon the Mask-RCNN architecture [25] as implemented in [26], due to its well-known detection capabilities. Mask-RCNN is modified to provide, for each detection bounding box, a specific feature descriptor to perform clustering afterwards. Inspired by the work of [27], we consider each object to be counted as approximable by a particular 2D shape. This assumption is embedded into the detector by training it on a novel 2D shape dataset, *InShape*.

InShape is a synthetic dataset of 50k images. Each one contains one or more basic shapes selected from the leaves of a 2D shape ontology inspired by [28]: *lined*, *triangle*, *rectangle*, *diamond*, *pentagon*, *hexagon*, *ellipse* (Fig. 2). For each shape, we generate instances by varying color (randomly in the RGB space) and scale (randomly from 5% to 20% of the image dimension). Instances of different shape classes are co-located in a single image in different spatial patterns (aligned with diverse geometrical layouts, or misaligned and following a Poisson spatial process). Images are made photorealistic (as they were taken from the real world as textural patterns) with the help of the Substance Designer tool (www.allegorithmic.com). Three *InShape* samples are shown in Fig. 3. Each image is annotated with bounding box coordinates and labels modeling the shape class, size and color for each object.

Mask-RCNN is modified by adding a new head branch dubbed *similarity head*, providing a similarity-based visual descriptor $desc(b)$ for each detection bounding box $b \in D$, where D is defined as the set of all the detected entities in the current training batch. This branch is placed after the bounding box regression branch of the Mask-RCNN model [25]. The $desc$ function is implemented as a 64-dimensional fully

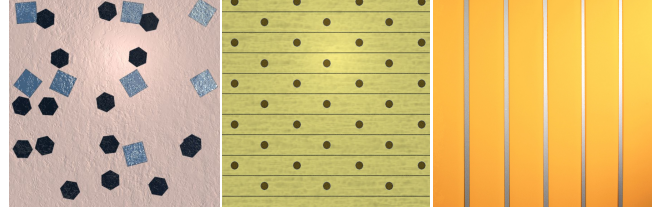


Fig. 3: *InShape* image samples. These samples show how different basic shapes are merged together in *InShape*. In a), two “types” of instances are present, dark gray hexagons and light gray squares; in b), circles and lines; in c), lines.

Same Image	Same Class	Same Type	P/N Pair
-	False	-	N
False	True	-	-
True	True	False	N
True	True	True	P

Table 1: Conditions for *negative* (N) and *positive* (P) pairs are indicated above. “Same Image” is true when two objects are in the same image; “Same Type” is true when color AND size are the same (“-” indicates that a value for that relation is not influencing the P/N Pair value).

connected layer from the RoI features corresponding to the computed box b . The output of this layer is constrained on the 64-dimensional hypersphere [29] (achieved by normalizing each embedding i.e. $\|desc(b)\|_2 = 1$).

We train this similarity-based descriptor so that: 1) instances of the same class (same basic shape) with the same color and scale (same “type”) are maximally close; 2) object instances of the same class with different color and/or scale or object instances of different classes have high distance. These two conditions are formally implemented as a triplet loss L_{sim} , and added to the Mask-RCNN loss as $L = L_{cls} + L_{box} + L_{mask} + L_{sim}$, with the first three terms being standard [26], while the new L_{sim} is defined as:

$$\sum_{\substack{(a,p) \in P \\ (a,n) \in N}} \max(\|desc(a) - desc(p)\|_2 - \|desc(a) - desc(n)\|_2 + \alpha, 0)$$

Above, P and N are respectively the set of positive detection pairs and the set of negative detection pairs, with $P, N \subseteq D \times D$; the definition of positive or negative object instance pairs is summarized in Table 1. One may note that during training the descriptors of each detection are compared not only within a single image, but also between detections belonging to different images in the same batch, according to the *Batch All* strategy as presented in [29, 30]. The training procedure follows the one presented in [25]. After the training on *InShape*, SIMCO can be applied to any image with no further fine-tuning. For a given test image, it produces a set of detection bounding boxes D (see Fig. 4 left), each one equipped with the related feature descriptor $desc(b)$ ($b \in D$).

2.2. SIMCO clustering

The embedding provided by the descriptor $desc(b)$ of Sec. 2.1 maps closely objects with the same shape and visual properties so that clustering can be applied to discover natural groupings. The idea is that each cluster is a “visual thing”.

As clustering procedure we choose the affinity propagation algorithm [23], since it exploits measures of similarity between pairs of data points (over which we had the Mask-RCNN loss computed) and simultaneously considers all data points as potential exemplars (specific representative of clusters). Affinity propagation has a single parameter (the *preference*) regulating the tendency to select less or more exemplars. By varying this parameter one can appreciate how the embedded features organize the detections (Fig. 4): starting from a low value and subsequently increasing it, drastically different scales are first separated (Fig. 4 in the center), followed by shape and color (Fig. 4 on the right).

3. EXPERIMENTS AND RESULTS

We evaluate single- and multi-class counting performances of SIMCO on the Cells [24] and RepTile [6] datasets and test it also on novel images to show diverse potential applications. Standard indexes of Mean Absolute Error (MAE) and Normalized Mean Absolute Error (NMAE) are evaluated [31]. In all of the experiments, SIMCO has the Mask-RCNN ResNet50-FPN [26, 32] as backbone architecture.

Cells counting. The Cells dataset [24] contains images of a single class of cells in challenging spatial configurations (variable density, occlusions); therefore, clustering is useless here and the detection capabilities of SIMCO can be fully highlighted. SIMCO counting performances on the Cells dataset are compared with those obtained by another recent object proposal model, *SharpMask* [33], and by the *Cai and Baci* [34] counting by detection algorithm. These are both single-class general-purpose automated approaches. To demonstrate the importance of using InShape for training we also report the results obtained training the same Mask-RCNN with COCO images.

Results are shown in Table 2, reporting also the running time on a NVIDIA GeForce GTX 1080 GPU. They show SIMCO definitely performing better than the alternatives. Results of [34] are poor due to the high spatial random displacements and the heavy occlusions of the Cells’ images; SharpMask scores closer to SIMCO, but behaves badly on occlusions. Mask-RCNN trained on COCO provides the worst counting accuracy scores. The running time further promotes SIMCO, with one tenth of second per image.

SIMCO on RepTile. To demonstrate the ability of SIMCO to count unknown objects of multiple classes we tested it on the RepTile dataset. RepTile is composed of 50 heterogeneous images (from hyperspectral imagery to aerial photos) with a total of 3173 annotated objects of varying and arbitrarily complex shapes (from candies to airplanes), taken

Method	Counting		Running Time (s)
	MAE	NMAE	
Cai and Baci [34]	149	0.809	753
SharpMask [33]	42	0.21	8.76
COCO/Mask-RCNN	175,65	0.99	0.12
SIMCO (no clustering)	12	0.07	0.11

Table 2: Counting results on Cells [24] dataset.

at different scales, illumination conditions etc. In addition, each image has a few specific types of objects annotated while other are not, in order to simulate a user which is interested only in some “things” in the image. This fits perfectly with the clustering parts of SIMCO. In particular, RepTile is thought for a human-in-the-loop approach, since each image has few “seed” detections, indicating the types of objects the user is interested to. For a fair comparison with the other alternative semi-supervised approaches using seed objects as input, we designed an automatic procedure to set the preference parameter based on the input seeds’ annotation. The procedure consists of increasing the preference parameter until each of the seed annotations is covered by a different cluster. Objects of these clusters are counted, while the others are discarded.

Compared methods are those of Cai and Baci [34], Arteta [24] and Setti [6], all exploiting the initial seed annotations (Cai and Baci can work both automatically as in the Cells test, and with supervision as required by the RepTile protocol). To demonstrate the advantages of clustering on our similarity branch output, we also report the results obtained with the affinity propagation clustering applied to the standard fully connected feature of the Mask-RCNN classification branch. Table 3 details how SIMCO produces a little more than half of the errors than Setti et al. [6], with ridiculously lower running time, definitely overcoming all of the other algorithms. Qualitatively, one may appreciate Fig. 4, showing the process of modulating the clustering until each of the desired seed detection was covered by a cluster; in particular for that image we stop at the second partition, being the yellow and the red fishes requested by the users. The same clustering procedure is not as effective when applied to the FC features of the classification branch (see Table 3).

SIMCO applications. Due to his high generalization and speed, SIMCO can be the engine for many useful and fancy tasks. SIMCO may help, in a picture, to answer visual questions related to counting, as in the case of Fig. 1. In many application domains, it can be used to solve hard multi-class clustering and counting problems, as shown in Fig. 5. In top row we see a complex mosaic of three types of bee cells, which SIMCO is able to precisely spot. In the middle row we show that SIMCO can handle also highly elongated shapes like fields partitions in remote sensing images, since InShape contains lines. In the bottom row we show the ability of the method to discriminate fine-grained classes of animals (e.g.

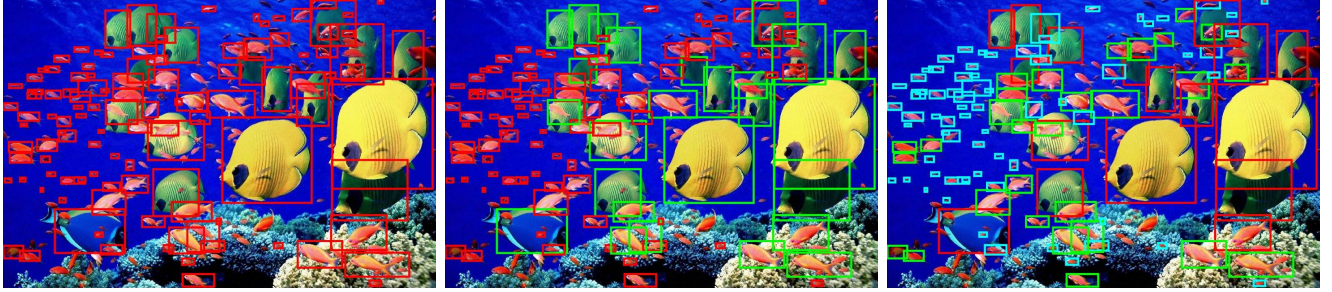


Fig. 4: SIMCO clustering process. By varying the preference value of the affinity propagation clustering, meaningful partitions are obtained. Left: results of the detection (no clustering). Center: the first separation individuates close and far fishes. Right: the second separation captures big circle-like fishes (red), foreground red fishes (green), background red fishes (cyan).

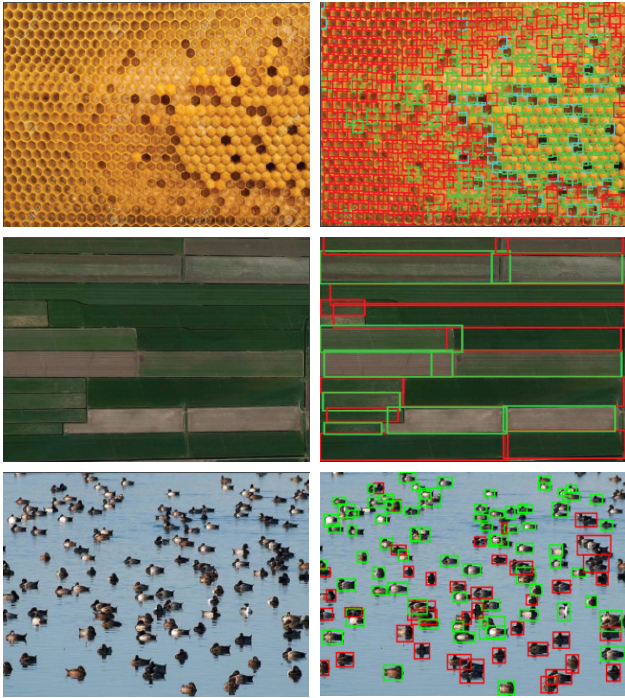


Fig. 5: SIMCO on challenging tasks. Top row: three types of cells are spotted. Middle row: highly elongated shapes such as light/dark green fields are correctly captured. Bottom row: *light and dark belly ducks* are separated into two clusters. This may help an annotator interested only in one of the two species. The high density of the mosaic of bee cells, the difficult shapes ratio in the second task and the fine-grained classes separation in the third further highlight the strengths of SIMCO.

light/dark belly ducks). This property can be used, in zoology or other domains, to develop user tools for image annotation aimed at training classifiers for very specific species (e.g., *light belly ducks*).

Finally, a photoediting example is shown in Fig. 6: a magic wand driven by SIMCO can select clusters of similar objects with very few clicks, so that they can be simultaneously removed and inpainted afterwards.

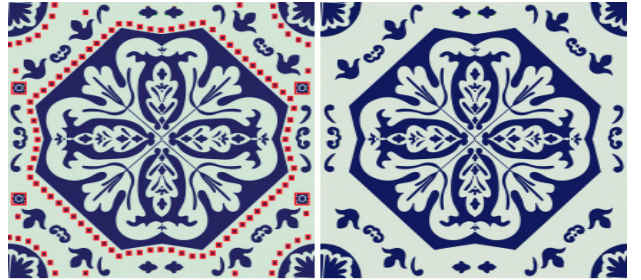


Fig. 6: Photoediting task. A magic wand based on SIMCO can select clusters objects to be removed (dots and flowers on the left). Selected objects can be removed with inpainting (right).

Method	Counting		Running Time (s)
	MAE	NMAE	
Cai and Baciú [34]	59	1.034	2814
Arteta et al. [24]	50	1.629	685
Setti et al. TM	18	0.186	-
Setti et al. TM + CE	18	0.164	-
Setti et al. complete [6]	14	0.109	867
COCO/Mask-RCNN/FC	46	0.521	0.18
InShape/Mask-RCNN/FC	19	0.272	0.18
SIMCO	8.66	0.086	0.18

Table 3: Counting results on RepTile [6] dataset, exploiting the protocol of [6].

4. CONCLUSION

We presented SIMCO, a powerful and flexible framework to select and count clusters of similar objects in images. An extensive experimental testing showed that the main ideas behind the method, e.g. training the detection on a custom dataset made of photorealistic images with repeated basic shapes (InShape) and learning an optimal embedding for elements’ clustering based on InShape annotations are particularly effective, making the framework suitable for a variety of practical applications in different domains.

5. REFERENCES

- [1] D. Kang, Z. Ma, and A. B. Chan, “Beyond counting: comparisons of density maps for crowd analysis tasks—counting, detection, and tracking,” *IEEE Transactions on Circuits and Systems for Video Technology*, 2018.
- [2] M. S. Norouzzadeh, A. Nguyen, M. Kosmala, A. Swanson, M. S. Palmer, C. Packer, and J. Clune, “Automatically identifying, counting, and describing wild animals in camera-trap images with deep learning,” *Proceedings of the National Academy of Sciences*, p. 201719367, 2018.
- [3] D. Onoro-Rubio and R. J. López-Sastre, “Towards perspective-free object counting with deep learning,” in *ECCV*, 2016.
- [4] T. Falk, D. Mai, R. Bensch, Ö. Çiçek, A. Abdulkadir, Y. Marrakchi, A. Böhm, J. Deubner, Z. Jäckel, K. Seiwald, et al., “U-net: deep learning for cell counting, detection, and morphometry,” *Nature methods*, p. 1, 2018.
- [5] E. Lu, W. Xie, and A. Zisserman, “Class-agnostic counting,” *arXiv preprint arXiv:1811.00472*, 2018.
- [6] F. Setti, D. Conigliaro, M. Tobanelli, and M. Cristani, “Count on me: learning to count on a single image,” *IEEE Transactions on Circuits and Systems for Video Technology*, 2018.
- [7] J. Zhang, S. Ma, M. Sameki, S. Sclaroff, M. Betke, Z. Lin, X. Shen, B. Price, and R. Mech, “Salient object subitizing,” in *CVPR*, 2015.
- [8] V. B. Subburaman, A. Descamps, and C. Carincotte, “Counting people in the crowd using a generic head detector,” in *2012 IEEE Ninth International Conference on Advanced Video and Signal-Based Surveillance*. IEEE, 2012, pp. 470–475.
- [9] A. Jabri, A. Joulin, and L. van der Maaten, “Revisiting visual question answering baselines,” in *ECCV*, 2016.
- [10] Y. Zhang, J. Hare, and A. Prügel-Bennett, “Learning to count objects in natural images for visual question answering,” *arXiv preprint arXiv:1802.05766*, 2018.
- [11] A. Agrawal, D. Batra, and D. Parikh, “Analyzing the behavior of visual question answering models,” *arXiv preprint arXiv:1606.07356*, 2016.
- [12] M. Noroozi, H. Pirsiavash, and P. Favaro, “Representation learning by learning to count,” in *ICCV*, 2017.
- [13] T. Katsuki, T. Morimura, and T. Idé, “Unsupervised object counting without object recognition,” in *ICPR*. IEEE, 2016.
- [14] M. Rucinski, “Modelling learning to count in humanoid robots,” 2014.
- [15] A. Cangelosi, A. Morse, A. Di Nuovo, M. Rucinski, F. Stramandinoli, D. Marocco, V. De La Cruz, and K. Fischer, “Embodied language and number learning in developmental robots,” *Conceptual and Interactive Embodiment: Foundations of Embodied Cognition*, vol. 2, pp. 275–293, 2016.
- [16] M. Andriluka, J. R. R. Uijlings, and V. Ferrari, “Fluid annotation: a human-machine collaboration interface for full image annotation,” *arXiv preprint arXiv:1806.07527*, 2018.
- [17] C. Spampinato, Y. Chen-Burger, G. Nadarajan, and R. B. Fisher, “Detecting, tracking and counting fish in low quality unconstrained underwater videos,” *VISAPP* (2), 2008.
- [18] A. Joly, H. Goëau, H. Glotin, C. Spampinato, P. Bonnet, W. Vellinga, J. Champ, R. Planqué, S. Palazzo, and H. Müller, “Lifeclef 2016: multimedia life species identification challenges,” in *International Conference of the Cross-Language Evaluation Forum for European Languages*. Springer, 2016.
- [19] A. Ferrari, S. Lombardi, and A. Signoroni, “Bacterial colony counting with convolutional neural networks in digital microbiology imaging,” *Pattern Recognition*, vol. 61, 2017.
- [20] T. Hollings, M. Burgman, M. van Andel, M. Gilbert, T. Robinson, and A. Robinson, “How do you find the green sheep? a critical review of the use of remotely sensed imagery to detect and count animals,” *Methods in Ecology and Evolution*, 2018.
- [21] E. Rosch, C. B. Mervis, W. D. Gray, D. M. Johnson, and P. Boyes-Braem, “Basic objects in natural categories,” *Cognitive psychology*, vol. 8, no. 3, pp. 382–439, 1976.
- [22] Z. Yan and X. S. Zhou, “How intelligent are convolutional neural networks?,” *arXiv preprint arXiv:1709.06126*, 2017.
- [23] B. J. Frey and D. Dueck, “Clustering by passing messages between data points,” *science*, vol. 315, no. 5814, pp. 972–976, 2007.
- [24] C. Arteta, V. Lempitsky, J. A. Noble, and A. Zisserman, “Interactive object counting,” in *European Conference on Computer Vision*. Springer, 2014, pp. 504–518.
- [25] K. He, G. Gkioxari, P. Dollár, and R. Girshick, “Mask r-cnn,” in *ICCV*. IEEE, 2017, pp. 2980–2988.

- [26] F. Massa and R. Girshick, “maskrcnn-benchmark: Fast, modular reference implementation of Instance Segmentation and Object Detection algorithms in PyTorch,” <https://github.com/facebookresearch/maskrcnn-benchmark>.
- [27] O. D. Faugeras and M. Hebert, “A 3-d recognition and positioning algorithm using geometrical matching between primitive surfaces,” in *IJCAI*. Morgan Kaufmann Publishers Inc., 1983, pp. 996–1002.
- [28] M. Niknam and C. Kemke, “Modeling shapes and graphics concepts in an ontology,” in *SHAPES*, 2011.
- [29] S. Ding, L. Lin, G. Wang, and H. Chao, “Deep feature learning with relative distance comparison for person re-identification,” *Pattern Recognition*, vol. 48, no. 10, pp. 2993–3003, 2015.
- [30] A. Hermans, L. Beyer, and B. Leibe, “In defense of the triplet loss for person re-identification,” *arXiv preprint arXiv:1703.07737*, 2017.
- [31] C. J. Willmott and K. Matsuura, “Advantages of the mean absolute error (mae) over the root mean square error (rmse) in assessing average model performance,” *Climate research*, 2005.
- [32] T. Lin, P. Dollár, R. Girshick, K. He, B. Hariharan, and S. Belongie, “Feature pyramid networks for object detection,” .
- [33] P. O. Pinheiro, T. Lin, R. Collobert, and P. Dollár, “Learning to refine object segments,” in *ECCV*. Springer, 2016.
- [34] Y. Cai and G. Baciú, “Detecting, grouping, and structure inference for invariant repetitive patterns in images,” *IEEE Transactions on Image Processing*, vol. 22, no. 6, pp. 2343–2355, 2013.